Science Advances

AAAS

advances.sciencemag.org/cgi/content/full/3/4/e1602402/DC1

Supplementary Materials for

Geochemical evidence for mélange melting in global arcs

Sune G. Nielsen and Horst R. Marschall

Published 7 April 2017, *Sci. Adv.* **3**, e1602402 (2017)
DOI: 10.1126/sciadv.1602402

This PDF file includes:

Supplementary Text

Additional arcs and data filtration

In the main paper we have chosen to illustrate mixing between mantle and sediment for three arcs only, due to space constraints. Tonga, Marianas and Lesser Antilles arcs were selected (Fig. 2), which are some of the best studied both in terms of the erupted lavas as well as characterization of the sediments and AOC outboard of the arcs. We have, however, compiled data for a total of eight arcs. In addition to the three displayed in the main manuscript, we also use the compiled data and model calculations presented in Nielsen *et al.* (*22*) for the Aleutians as well as data compiled from the Georoc database (http://georoc.mpch-mainz.gwdg.de) for the Kurile, Ryukyu, Scotia and the Java portion of the Sunda arc.

For every arc we have filtered the lava data and only included lavas from the main volcanic front. We also excluded samples with more than 62 % SiO_2 in order to avoid significant effects from assimilation and/or fractional crystallization. It is likely that some lavas will have experienced some fractional crystallization that can affect trace element ratios. In particular, plagioclase crystallization will remove Sr relative to Nd and increase Nd/Sr ratios compared with the primitive lava (Fig. 2). Thus, some of the highest Nd/Sr ratios in Fig. 2d–f are likely not related to processes occurring in the mantle wedge, but reflect shallower processes. This effect only reinforces the observation that Nd/Sr ratios in a large portion of arc lavas are too low to realistically be explained by sediment melts and AOC fluids (Fig. 2d–f). Isotope compositions, however, are unaffected by fractional crystallization and thus only substantial amounts of crustal assimilation would affect the Sr and Nd isotope compositions. We conclude that the effects of assimilation are likely very minor because none of the filtered data sets display co-variation between, for example, SiO_2 or absolute trace element concentrations and the Sr and Nd isotope compositions (not shown). Based on these arguments we infer that the isotope data for arc lavas (Fig. 2a–c and fig. S2) broadly represent compositions extracted from the mantle and do not reflect shallow crustal processing.

Determination of bulk sediment, AOC and mantle compositions

For each arc (Fig. 2 and fig. S2) we have investigated the Nd and Sr isotope compositions and concentrations for the local subducting sediment and the mantle wedge. Where available, we have also added data for AOC. All the utilized endmember compositions and the primary references used to deduce these values are shown in table S1. In general, we have relied heavily on the seminal work by Plank and Langmuir (*37*) who investigated the compositions of the sediment subducted underneath all the arcs compiled here except the Ryukyu arc. Most of the sediment concentration data are taken from Plank and Langmuir (*37*), with additional data from Nielsen *et al.* (*22*) and Vervoort *et al.* (*38*). For some arcs additional sediment isotope composition data has recently become available (*22, 38, 39*) and we have combined these newer data with those presented in Plank and Langmuir (*37*) to form more robust average sediment compositions. In some arcs, previous work has identified two geographically distinct sediment compositions (for example pelagic and terrigenous sediments that dominate the Central and Eastern Aleutians, respectively (*22*) and we, therefore, used two sediment components in these arcs (table S1).

For AOC compositions we have used literature compilations of average AOC compositions in drill holes proximal to some of the arcs. However, such data are only available for three of the eight arcs investigated here (table S1).

The Sr and Nd concentration of the mantle wedge is always assumed to be identical to the estimate for the depleted mid ocean ridge basalt mantle (DMM) presented by Salters and Stracke(*40*). The absolute concentration of the unmodified mantle wedge in different arcs might vary significantly due to different degrees of melt depletion. However, because Sr and Nd partition similarly during mantle melting (*41*) the Sr/Nd ratio of the unmodified mantle wedge is unlikely to vary much and, therefore, the curvature of all the mixing lines are the same irrespective of the absolute Sr and Nd concentrations in the mantle wedge. The only effect of altering the mantle wedge Sr and Nd concentrations would be the amount of sediment needed to obtain a given Nd and Sr isotope composition. The Sr and Nd isotope compositions of global mid ocean ridge basalts (MORB) display strong co-variation (*42*), which implies that the mantle wedge will follow this relationship. Thus, any uncertainties in Sr or Nd isotope compositions

estimated for the mantle wedge are correlated. A significantly lower estimate for the $^{144}Nd/^{143}Nd$ ratio for the mantle wedge realistically has to accept a higher estimate for its $^{87}Sr/^{86}Sr$ ratio and we have indicated the potential Sr and Nd isotope variation of the mantle wedge with an error ellipse in Fig. 2 and fig. S2 around the mantle compositions. The arc lava compositions would consequently remain scattered around the mantle–bulk sediment mixing lines and no solution can be found for which the mantle–sediment partial melt mixing lines follow the arc lava data. Our conclusions, therefore, remain valid irrespective of the choice of the mantle wedge isotopic composition. Nevertheless, given that each of our estimates for the mantle wedge fall close to the apex of the respective arc lava data (Fig. 2a–c and fig. S2), we are confident that our mantle wedge estimates are accurate.

Below we briefly describe how we arrive at the Nd and Sr isotope compositions for each component summarized in table S1.

Aleutian arc

The recent study by Nielsen *et al.* (*22*) has shown that two distinct sediment components are present in Aleutian lavas east of Kanaga Island. Lavas erupted further west in the Aleutians are affected by very slow subduction rates and potentially reflect slab melting (*43*). The Western Aleutians are, therefore, not considered in this literature compilation. Of the two sediment components in the Central and Eastern Aleutians, one is pelagic sediment with a significant amount of authigenic Fe-Mn oxyhydroxides that is dominant in the Central Aleutians. These sediments are represented by the average composition in ODP Hole 886C (*22*). The other sediment component is largely terrigenous and originates from the North American continent and is represented by DSDP Holes 178 and 183 (*37*). Additional Nd isotope data from DSDP Holes 178 and 183 (*38*) are in good agreement with the previous estimate (*37*) that was based on much fewer analyses.

For the mantle isotope composition we have used the most proximal MORB sample, which is located on the northern Juan de Fuca Ridge (*44*).

Kurile arc

For the sediment, we have adopted the Sr and Nd concentrations and Sr isotope composition presented in Plank and Langmuir (*37*). Recent Nd isotope data from ODP Site 881 located outboard of the northern end of the Kurile arc (*38*) reveal slightly more radiogenic data than the previous estimate (*37*) so we have made a revised estimate for the Nd isotope composition of Kurile sediments of $^{143}Nd/^{144}Nd = 0.5124$ (table S1).

The mantle wedge composition of the Kurile arc is not easily constrained with proximal samples so we have used the value for average Pacific MORB of $^{143}Nd/^{144}Nd = 0.5132$ and $^{87}Sr/^{86}Sr = 0.7025$ (*42*).

Lesser Antilles arc

The Lesser Antilles arc comprises two distinct sediment sources: Pelagic/volcaniclastic sediments in the north and terrigenous sediments from the Orinoco delta in the south. DSDP Site 543 represents the northern sediments (*37*), while we use the average composition of six piston cores in terrigenous sediment outboard of the Lesser Antilles arc (*45*) as the best estimate for the southern Antilles sediments. No deep sediment drilling has ever been performed in the southern Lesser Antilles and, therefore, this composition is associated with significant uncertainty.

The AOC subducted under the Lesser Antilles is inferred to be similar to the supercomposite of DSDP Sites 417/418 (*46*), which are located to the north of the Lesser Antilles.

The mantle wedge in the Lesser Antilles is estimated to be similar to average Atlantic MORB (*42*).

Mariana arc

The average Sr and Nd concentration and Sr isotope sediment composition is from Plank and Langmuir (*37*). Recently published Nd isotope data (*38*) have shown that some of the sediment units are somewhat less radiogenic than initially estimated by Plank and Langmuir (*37*). We have, therefore, revised the Nd isotope composition of Mariana sediments down to $^{143}Nd/^{144}Nd = 0.5124$ (table S1).

The Sr and Nd concentrations and isotope compositions of AOC is the average of Site 801 estimated by Hauff *et al.* (*47*).

The mantle wedge for the Mariana arc was estimated by using the most MORB-like samples found in the Mariana Trough (*48*, *49*).

Ryukyu arc

No compilation of sediment data outboard of the Ryukyu arc exists. Recent Nd concentration and isotope data for DSDP Site 294 and 295 showed an average Nd concentration of 67 μg/g and $^{143}Nd/^{144}Nd$ ~ 0.51238 (*38*). In order to further characterize the Sr and Nd isotope compositions of sediment and AOC input to the Ryukyu arc we here present 6 new Sr and Nd isotope measurements for pelagic sediments recovered from DSDP Holes 294 and 295 and 7 AOC samples recovered from DSDP Holes 442B and 294 (table S2). Analytical methods for determination of isotope compositions and concentrations followed those described previously (*22*). The sediment samples were selected to represent all lithologies present in these drill cores such that we could reconstruct a mass-weighted average Sr and Nd isotope composition and concentration for Ryukyu subducted sediments. All sediment isotope data, except one Nd isotope analysis, fall within relatively narrow ranges of $^{87}Sr/^{86}Sr$ ~ 0.7086-0.7121 and $^{143}Nd/^{144}Nd$ ~ 0.51232–0.51241. The mass-weighted average isotope compositions are $^{87}Sr/^{86}Sr$ ~ 0.7090 and $^{143}Nd/^{144}Nd$ ~ 0.51240 where the Nd isotope composition is identical to the data presented in Vervoort *et al*. (*38*). The mass-weighted average Nd concentration of the subducted sediment is 61μg/g, which is very similar to the average concentration found in Vervoort *et al*. (*38*) of 67μg/g. The mass-weighted Sr concentration of the Ryukyu sediments was found to be 300μg/g, which is also reasonably close to the previous estimate that was based only on sediments outboard of the Mariana arc (*37*).

For the AOC, we analyzed six samples from DSDP Hole 442B and one from DSDP Hole 294 that display limited Sr and Nd isotope variation and we use the average composition of these samples to characterize the subducted AOC component.

The mantle wedge is assumed to be similar to Indian MORB (*42*), which is similar to what has been inferred in previous studies (*50*).

Scotia arc

The average Sr and Nd concentration and Sr isotope sediment composition is from Plank and Langmuir (*37*). Recently published Nd isotope data (*38*) have shown that some of the sediment units are slightly less radiogenic than initially estimated by Plank and Langmuir (*37*). We have, therefore, revised the Nd isotope composition of Scotia arc sediments down to $^{143}Nd/^{144}Nd$ = 0.5123 (table S1).

The mantle wedge for the Scotia arc was estimated by using the most MORB-like samples found on the East Scotia Ridge (*51*).

Sunda arc (Java)

Sediment cores from DSDP Sites 211 and 261 have shown that three units are present outboard of the Java portion of the Sunda arc: 1) Pelagic clay, 2) biogenic clay, 3) Nicobar turbidites. The average Sr and Nd concentrations of the total sediment column are 218 μg/g and 34 μg/g, respectively (*37*). Here we estimate the isotope compositions of each sediment unit using the piston core data of Ben Othmann *et al*. (*45*) as well as the Nd isotope compositions of sediments from DSDP 211(*38*). These data provides the following compositions for each unit: 1) $^{143}Nd/^{144}Nd$ = 0.512163, $^{87}Sr/^{86}Sr$ = 0.71682, 2) $^{143}Nd/^{144}Nd$ = 0.512378, $^{87}Sr/^{86}Sr$ = 0.70916, 3) $^{143}Nd/^{144}Nd$ = 0.51195, $^{87}Sr/^{86}Sr$ = 0.70802. We weight each sediment unit according to the lithological thickness and density provided by Plank and Langmuir (*37*) and obtain an average sediment composition of $^{143}Nd/^{144}Nd$ = 0.51222, $^{87}Sr/^{86}Sr$ = 0.7129 (table S1).

The composition of AOC is inferred to be represented by basaltic crust drilled at ODP Sites 757 and 758 and DSDP Site 214 all on the Ninetyeast Ridge (*52–54*).

The Sr and Nd isotope compositions of the mantle wedge are assumed similar to average Indian Ocean MORB (*42*).

Tonga arc

There are two distinct sediment components subducting underneath the Tonga arc: 1) pelagic sediments that are represented by DSDP Sites 595 and 596 (*37*) and 2) Volcaniclastic sediments sourced from the Louisville Seamounts that are abundant in sediments from DSDP site 204 (*39*). We use the average Sr and Nd concentrations for the pelagic sediments provided by Plank and Langmuir (*37*), while Sr and Nd isotope compositions for the pelagic clays are from Ewart *et al.* (*39*) and Vervoort *et al*. (*38*), respectively. The volcaniclastic sediments from Site 204 are taken from Ewart *et al*. (*39*) and we simply use the average composition for the four volcaniclastic sediments analyzed there.

The mantle wedge composition is estimated from the most depleted samples found in the Eastern Lau Spreading Center and the Valu Fa Ridge (*55, 56*).

fig. S1. Mixing diagrams between sediments and mantle for Kurile, Ryukyu, Scotia, Aleutian, and Sunda arcs. Plots of Sr isotopes against Nd isotopes (a-e) and Nd/Sr ratio (f) for lavas from the Ryukyu (a), Sunda (b), Aleutians (c and f), Scotia (d) and Kurile (e) arcs. Literature data from the Georoc database (http://georoc.mpch-mainz.gwdg.de/georoc/) and only recent subaerial extrusive lavas with <62 % SiO_2 have been included to avoid effects from fractional crystallization and assimilation (see supplement for details). Details of the mantle, sediment and AOC end-member compositions can also be found in the supplement. Mixing lines between mantle and bulk sediment (bold lines), 1 % partial sediment melts (dashed lines), and 20 % partial sediment melts (dotted lines) show different curvature, because Nd/Sr ratios fractionate strongly during sediment partial melting (*8, 14*). Additional mixing lines between the mantle and AOC fluids (pink bold lines) and 1% partial sediment melts and 1% by weight AOC fluids (pink dashed lines) are also shown for arcs where the AOC component is constrained. Tick marks on individual mixing curves indicate the amount in weight percent of bulk sediment or sediment melt that is added to the mantle. The partition coefficients for Sr and Nd during sediment melting were set to D_{Sr} = 7.3 and D_{Nd} = 0.35, which represents the average values recorded in sediment melting experiments by Hermann and Rubatto (*14*) over the temperature range 750-900°C. Partition coefficients for AOC fluids were set to D_{Sr} = 2 and D_{Nd} = 0.15, which represents the values found for 800°C and 4GPa (*13*). The Nd/Sr ratio of AOC fluids in (f) are

not quantified, but conservatively inferred close to 0 in order to explore the largest possible effect from AOC fluid addition (see text for details).

fig. S2. Plots of SiO_2 against Sr isotopes for arc lavas from all 8 arcs investigated in this study. All data from the Georoc database (http://georoc.mpch-mainz.gwdg.de/georoc/). It is evident that lavas with higher SiO_2 contents are not associated with more radiogenic Sr isotope compositions as would be expected from significant crustal assimilation. We, therefore, conclude that the vast majority of radiogenic isotope variation in the selected arc lavas result from slab material in the arc lava source region.

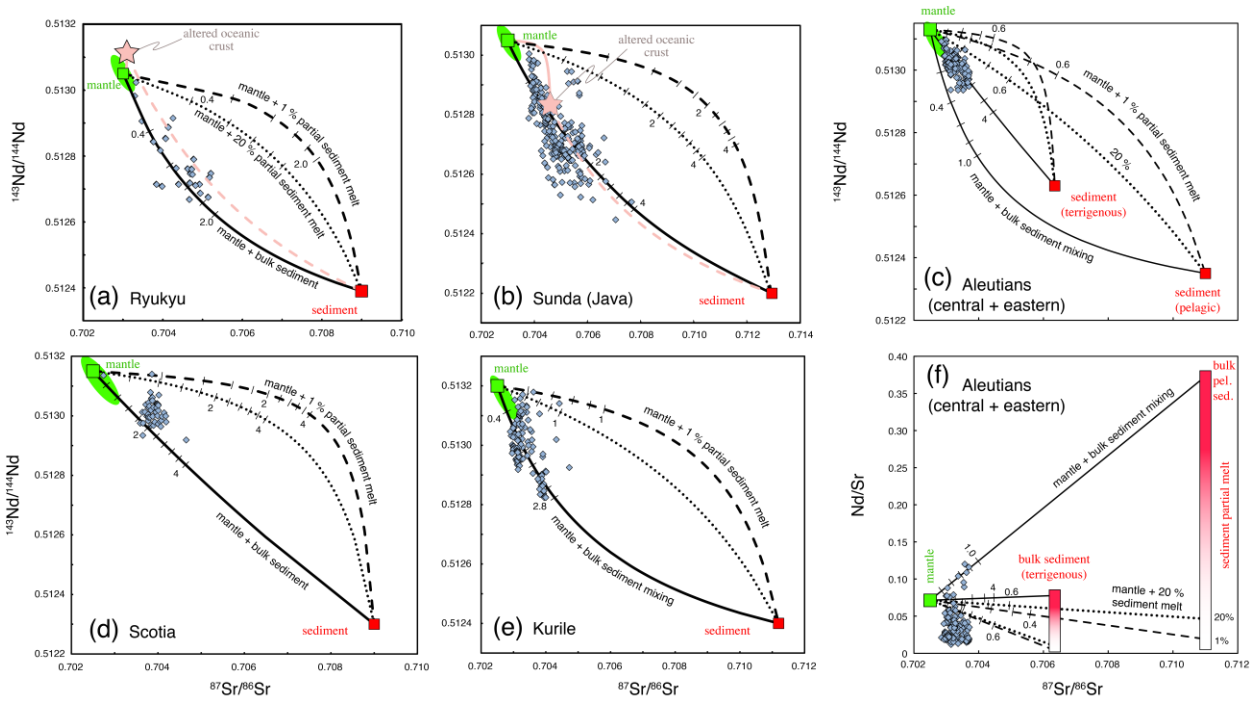

fig. S1. Mixing diagrams between sediments and mantle for Kurile, Ryukyu, Scotia, Aleutian, and Sunda arcs.

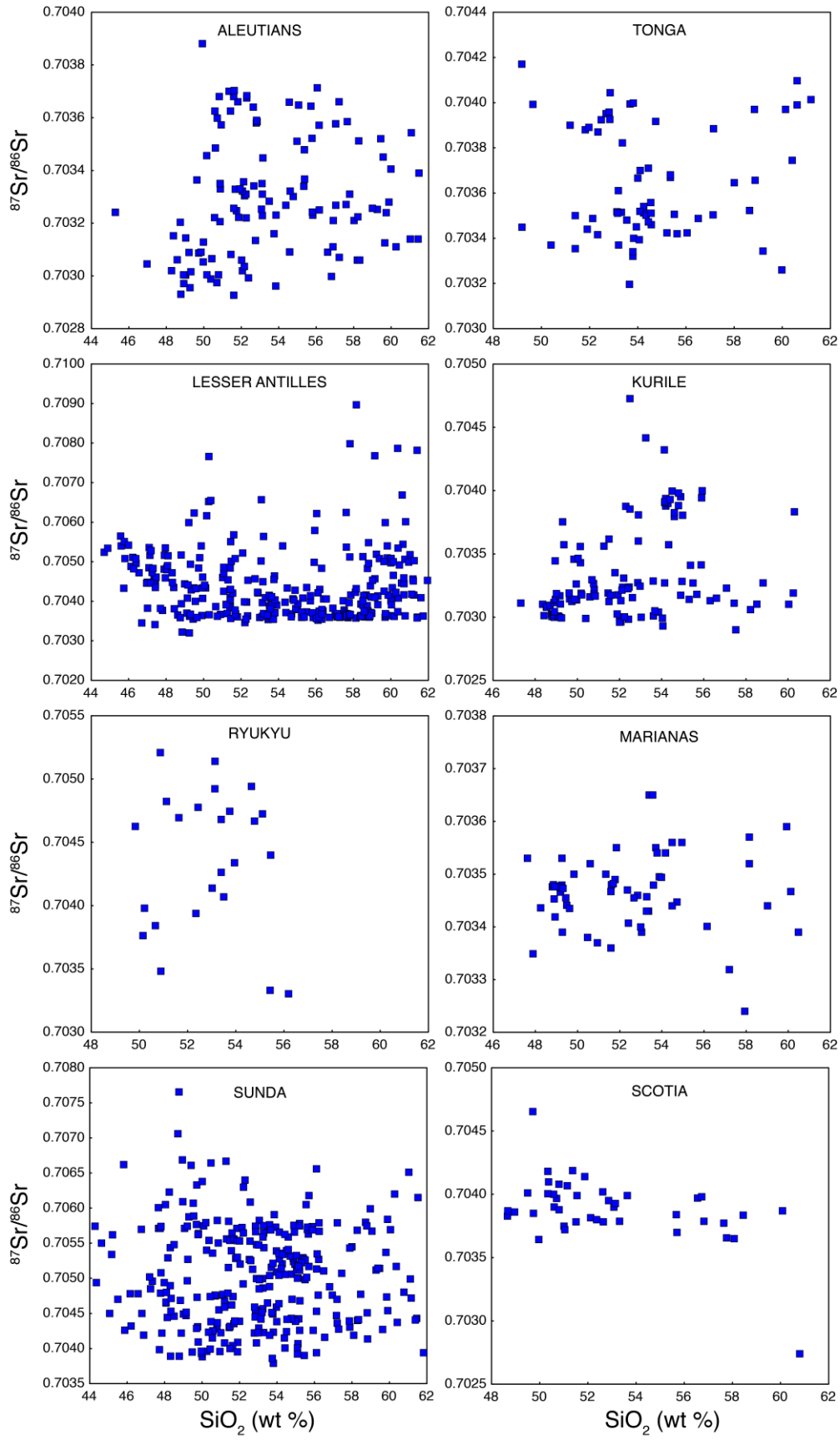
ALEUTIANS
TONGA
LESSER ANTILLES
KURILE
RYUKYU
MARIANAS
SUNDA
SCOTIA
$^{87}Sr/^{86}Sr$
SiO_2 (wt %)

fig. S2. Plots of SiO_2 against Sr isotopes for arc lavas from all eight arcs investigated in this study.

table S1. Compositions of endmember mixing components in Fig. 2 and fig. S1.

	Mantle				Sediment 1				Sediment 2				AOC			
Arc	[Sr]	[Nd]	$^{87}Sr/^{86}Sr$	$^{143}Nd/^{144}Nd$	[Sr]	[Nd]	$^{87}Sr/^{86}Sr$	$^{143}Nd/^{144}Nd$	[Sr]	[Nd]	$^{87}Sr/^{86}Sr$	$^{143}Nd/^{144}Nd$	[Sr]	[Nd]	$^{87}Sr/^{86}Sr$	$^{143}Nd/^{144}Nd$
Aleutians	9.8	0.713	0.7025	0.51313	245	19	0.7064	0.51263	203	76	0.7110	0.51235				
Kurile	9.8	0.713	0.7025	0.5132	87	22	0.7112	0.51240								
Lesser Antilles	9.8	0.713	0.7025	0.51315	110	31	0.7179	0.51190	237	35	0.7138	0.51206	180	6.7	0.7046	0.51308
Mariana	9.8	0.713	0.7027	0.51315	161	21	0.7070	0.51240					119	10	0.7044	0.51307
Ryukyu	9.8	0.713	0.7030	0.51305	300	61	0.7090	0.51239					160	10	0.7031	0.51311
Scotia	9.8	0.713	0.7025	0.51315	115	10	0.7090	0.51230								
Sunda/Java	9.8	0.713	0.7030	0.51305	218	34	0.7129	0.51222					166	7	0.7046	0.51283
Tonga	9.8	0.713	0.7032	0.51315	163	19	0.7064	0.51280	233	158	0.7091	0.51235				

Mantle composition based on data in (40, 42, 44, 48, 49, 50, 51, 55, 56)

Sediment compositions based on data in Table S2 and (22, 35, 37, 38, 39, 45)

AOC compositions based on data in Table S2 and (46, 47, 52, 53, 54)

table S2. Strontium and neodymium isotype compositions for sediments and altered basalts in front of the Ryukyu arc.

Site	Core	Section	Interval (cm)	Hole Depth (m)	Description	87Sr/86Sr	Sr (ppm)	143Nd/144Nd	Nd (ppm)
Sediments									
294	1	1	122-124	1.22-1.24	Brown silt-rich clay	0.71120	109	0.51234	18.3
294	3	4	63-65	79.13-79.15	Dusky brown clay	0.70890	100	0.51242	31.0
294	4	3	70-72	96.7-96.72	Dusky brown clay	0.70844	429	0.51238	147.4
294	6	1	72-74	106.22-106.24	Blackish red ferruginous silt-rich clay	0.70830	615	0.51272	82.1
295	1	4	74-76	106.24-106.26	Brown clay	0.71215	150	0.51233	30.2
295	3	3	80-82	142.8-142.82	Dusky brown ferruginous zeolite-rich silty clay	0.70862	569	0.51235	68.4
Altered basalts									
294	7	1	147-149	113.47-113.49	Interstitial tholeiitic basalt	0.70412	367	0.51290	32.5
442B	4	2	81-83	298.31-298.33	Aphyric, vesicular basalt	0.70319	156	0.51312	8.6
442B	8	5	71.5-73.5	340.025-340.045	Aphyric, vesicular basalt	0.70304	146	0.51313	8.0
442B	11	1	64-66	363.14-363.16	Aphyric pillow basalt	0.70328	165	0.51311	11.0
442B	16	1	81-83	410.81-410.83	Aphyric pillow basalt	0.70326	217	0.51308	13.6
442B	17	1	79-81	417.79-417.81	Aphyric, pillow basalt	0.70298	166	0.51312	11.9
442B	19	2	40-42	437.9-437.92	Aphyric, pillow basalt	0.70294	155	0.51314	10.4